

Analog to Digital Microfluidic Converter

Renaud Dufour, Chang Wu, Farida Bendriaa, Vincent Thomy and Vincent Senez*

BioMEMS Group, IEMN (UMR 8520 - University of Lille Nord de France)

*BP 60069, Avenue Poincaré, 59652 Villeneuve d'Ascq cedex, France – vincent.senez@isen.fr

Abstract: This paper presents an Analog to Digital Microfluidic Converter (ADMC) using passive valves and enabling the conversion of a continuous liquid flow into droplets for electrowetting on dielectric (EWOD) actuation. Valves calibration, geometry characteristics and losses reduction have been optimized using microfluidic application mode of COMSOL Multiphysics.

Keywords: EWOD, Lab-on-chip, microfluidic.

1. Introduction

Microfluidic devices can handle tiny volumes of liquid as either continuous flows in micro-channels or droplets on hydrophobic surfaces. Up to now, most lab-on-chips (LOC) have been implemented with only one of these two technologies. However, by analogy with microelectronic systems, one can easily understand that, depending on operations, both technologies have their own advantages and drawbacks. As a consequence, systems that can convert a continuous flow into droplets and, reciprocally, that can convert droplets into continuous flows have to be studied. Thanks to numerical simulations using COMSOL Multiphysics, we have designed an analog (continuous flow) to digital (droplet displacement) microfluidic converter (ADMC). The second section of this paper describes the numerical model and its calibration, the third section is devoted to the design of the ADCM and the analysis of the simulations.

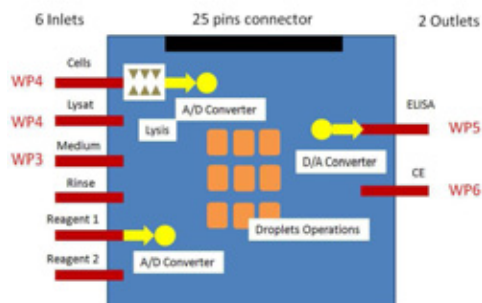


Figure 1. Microfluidic multiplexer integrating both analog and digital microfluidics.

Figure 1 gives a schematic example of a system incorporating AD/DA microfluidic converters as envisioned in the European FP7 project NANOBE [1]. In this system, the manipulation of the droplets is performed by dynamic modification of the wettability of the surfaces thanks to EWOD concept [2]. Figure 2 presents four snapshots of an experiment where a droplet is generated from a capillary and then moved by electrowetting actuation. However, this direct connection between continuous flow (capillary or micro-channel) and EWOD network presents two major drawbacks: there is no droplet-volume control, and we cannot evacuate liquid excess in case of overpressure. This is the reason why an efficient analog to digital microfluidic interface has to be studied.

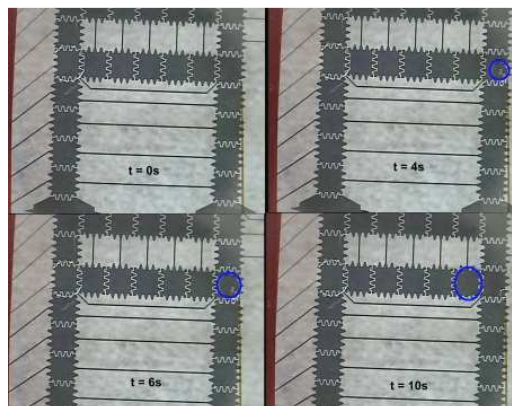


Figure 2. EWOD device: electrodes are 2mm x 2mm in size, 1.4 μ L droplet is created from a capillary (inside diameter 75 μ m) and moved under 100V at 1 kHz.

2. Modeling and calibration

Our first tests have been performed to assess the accuracy of the numerical modeling for a simple case. A micro-channel is filled with liquid applying a constant pressure at the inlet and taking into account capillary effects. Figure 3 gives the variation of the liquid/air interface as a function of time obtained by the COMSOL simulations (dotted line). This result is compared with the analytical models of Washburn (green

line) [3] and Zeng (red line) [4]. One can observe a good agreement between the numerical and analytical results. This first study demonstrated the reliability of the simulation concerning dynamic of capillary filling for a simple geometry and enabled modeling of a more complex microfluidic network.

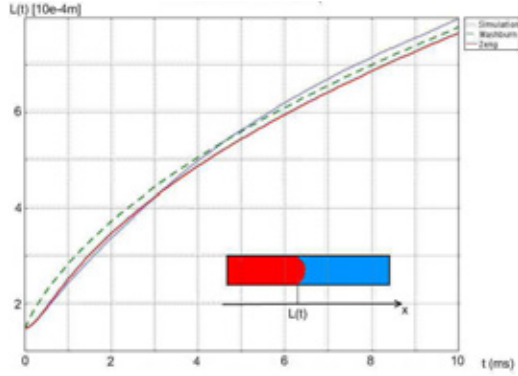


Figure 3. Micro-channel filling : interface position $L(t)$ as a function of time. Numerical results (blue dotted line), Washburn model (green) and Zeng (red).

Our ADMC is based on passive valves to control liquid flow [5]. A passive valve is a modulation of the channel geometry. It is described by two parameters: the channel width (W_1) and the valve width (W_2) (see inset of Figure 4). We use rounded geometry to avoid losses at the corners and channels thickness is $200\mu\text{m}$. Using the Laplace law, we find that the pressure barrier at the valve inlet is given by:

$$\Delta P = -2\sigma\cos(\theta)\left(\frac{1}{W_2} - \frac{1}{W_1}\right) \quad (1)$$

With σ the surface tension and θ the wall contact angle (top and bottom plates contact angles are not involved as the modulation is only widthwise). Moreover, considering $W_1 \gg W_2$ (channel width remains the same and is much larger than valves width), the pressure barrier increases with $\frac{1}{W_2}$ (figure 5).

2.1 Use of COMSOL Multiphysics

Numerically, the problem consists in a laminar two-phase flow in a variable cross-section micro-channel, considering capillary effects. We use the “Two-phase flow, phase

field” COMSOL application mode, which enables 3D interface tracking and contact angle specification to simulate the operating cycle of this device, filled by water at constant flow rate ($100\mu\text{L}/\text{min}$). Level set application mode has also been used since in our case the ‘phase field’ method converges more easily. Wetted-wall boundary conditions are used ($\theta = 100^\circ$ for the walls and 110° for top and bottom plates), with laminar inflow and outlet constant pressure ($1e5$ Pa). We need to know ΔP according to valve geometry, so we observe computed pressure variation which maintains the flow rate constant.

2.2 Passive valves calibration

Inlet pressure variations versus time are shown on Figure 4. First, liquid fills up the large channel of width W_1 and pressure increases very little up to $t = 0.4\text{s}$ (because of the pressure drop from the inlet to the moving interface, characterizing a laminar flow); then as the interface reaches the end of this first channel, a pseudo hydrophilic effect due to curvature reversal is observed (see bottom inset of figure 4: curvature changes while contact angle on the wall does not). Positive pressure drop is observed as the liquid enter the valve. Indeed, capillary resistance is larger in the narrow channel, so a larger pressure is needed to keep the flow rate constant. A pressure overshoot is noted as the liquid get out the valve because at the exit curvature become even larger.

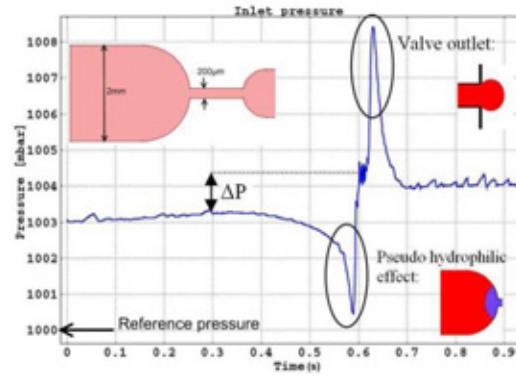


Figure 4. Single passive valve simulation: inlet pressure as a function of time.

Eventually, pressure becomes constant again when the liquid flows in the second part of the valve. Pressure barrier corresponds to the difference between pressure in the first channel and pressure inside the valve: here $\Delta P = 1,15\text{mbar}$. Figure 5 shows the variation of the pressure barrier versus valve width obtained either by the numerical simulation (red diamonds) or by the analytical model (black full line) given above. One can observe the good agreement between them. Besides this results points out that, if we consider channels of a few millimeters in width, valves width should be narrower than $200\ \mu\text{m}$ in order to obtain a sufficient pressure barrier (more than 1 mbar).

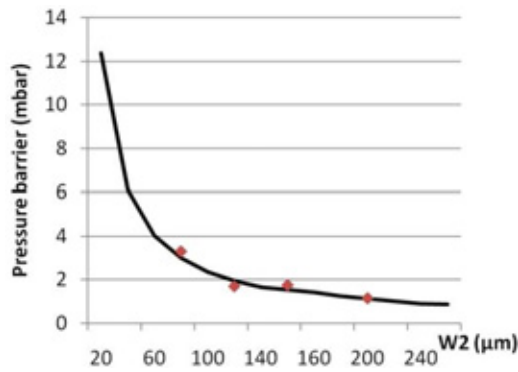


Figure 5. Pressure barrier as a function of valve parameters for $W_1=2\text{mm}$. Analytical solution (solid line, refers to equation 2.1) and computed results (red diamonds). Last diamond corresponds to the valve characteristic on figure 4.

3. ADMC device design

From this simplified study, we have designed our ADMC device (figure 6): a $200\ \mu\text{m}$ thick micro-channels network. The geometrical features of the inlet capillary are: diameter ($75\ \mu\text{m}$), length (5cm), inlet pressure (1bar or $80\ \mu\text{L}/\text{min}$ water flow-rate). Three passive valves ($V1 < V2 < V3$) are integrated in the device. As $V1 < V2$, the inlet liquid-flow fills up a $1\ \mu\text{L}$ cavity and is stopped by $V3$. Then, since $V2 < V3$, liquid excess is evacuated to the waste channel. Eventually, a $1\ \mu\text{L}$ droplet is generated on the EWOD electrode activating an air inlet located at $V1$ and setting the contact angle on the EWOD electrode at 80° (hydrophilic surface).

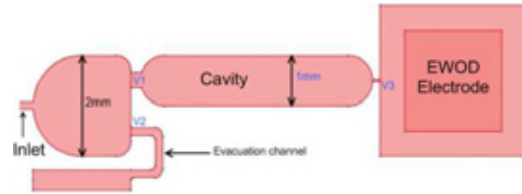


Figure 6. Microsystem (top view).

3.1 Simulation

Outlets pressure is set at $1e5\text{Pa}$. Wetted-wall boundary condition is used for walls ($\theta_w = 100^\circ$), top and bottom plates ($\theta_p = 110^\circ$). Continuity condition is applied to initial fluid interface. COMSOL simulations are performed to optimize the valves dimensions and positions in order to improve the filling of the cavity and to decrease losses in the evacuation channel. Air inlet positioning and pressures have to be also optimized to obtain optimal emptying of the cavity and to avoid air bubbles inside water. In our simulations, the mesh is composed of 30.000 elements. Anisotropic artificial diffusion is set. After interface initialization, 500.000 DOFs are computed using PARDISO solver and while time steps (seconds) are $0:0.001:3$. Computation time is approximately 100 hours on a Sun workstation.

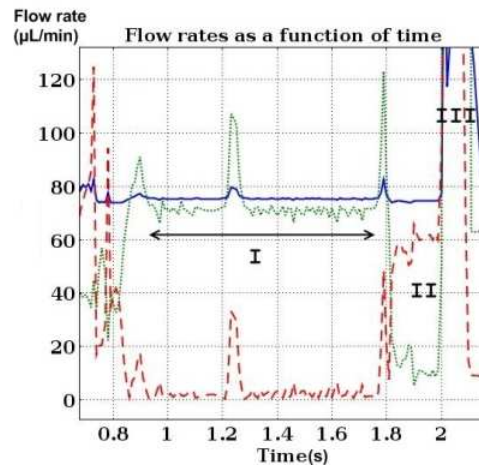


Figure 7. Inlet, cavity and waste flow-rates (respectively in blue, green and red) as a function of time: I - Cavity filling, waste flow rate = 0; II - Cavity is full: there is a reversal of waste and cavity flow-rates; III - Air inlet is enabled and cavity is evacuated at higher flow rate ($600\ \mu\text{L}/\text{min}$ for 0.1s).

3.2 Results

Figure 7 gives the variations of the flow rates (computed using boundary integration) versus time. It is clearly shown that during cavity filling ($0.9 < t(s) < 1.8$), waste flow rate is very small, whereas it becomes equal to inlet flow rate as soon as the cavity is full, because the liquid is stopped by V3. Thus for $1.8 < t(s) < 2$, liquid excess flows through the evacuation channel. Eventually when air inlet (located at V3) is activated (air pressure is 1 bar), the cavity is emptied and the $1\mu\text{L}$ droplet is created on the EWOD electrode. We find again some pressure variations due to pseudo hydrophilic effects, caused by rounded geometry. Figure 8 gives various snap-shots of the simulation during its operation cycle. During droplet generation, $0.2\mu\text{L}$ of liquid flows through the evacuation channel ($140\mu\text{L}/\text{min}$ for 0.1s), which corresponds to 20% liquid lost, so 80% of the continuous flow is converted into droplets.

4. Conclusions

As a conclusion, simulations with COMSOL have enabled the development of an ADMC device fully compatible with EWOD technology. It allows us to integrate both continuous and digital microfluidic on the same chip by converting a fluid flow into constant-volume droplets. Actually losses are not negligible but it is possible to decrease them considerably using more than one cavity, and so creating multiple droplets at the same time. Following this work, we are actually developing a microtechnological process to include this ADMC in our EWOD chip.

5. Acknowledgments

Part of this work has been carried out within the NANOBE project funded by the European Commission.

6. References

1. "Nano and microtechnology based analytical devices for online measurements of bioprocesses" NANOBE project, STREP FP7 project, 04/2009-03/2012, KBBE20083203 Nanobiotechnology based

biosensors for optimized bioprocesses (http://cordis.europa.eu/fetch?CALLER=FP7_PROJ_EN&ACTION=D&DOC=33&CAT=PROJ&QUERY=0121e3b6b79d:7fe5:6118d82a&RCN=90335).

2. R.B. Fair, Digital microfluidics: is a true lab-on-a-chip possible? *Microfluid Nanofluid*, **3**, 245-281(2007).
3. E.W. Washburn, The dynamics of capillary flow, *Physical review*, **17(3)**, 273-283(1921).
4. J. Zeng, On modeling of capillary filling, http://www.coventor.com/pdfs/on_modeling_of_capillary_filling.pdf (2007).
5. Chong H. Ahn et al, Disposable smart Lab on a Chip for Point-of-care Clinical Diagnostics, *Proceedings of the IEEE*, **92(1)**, 154-173(2004).

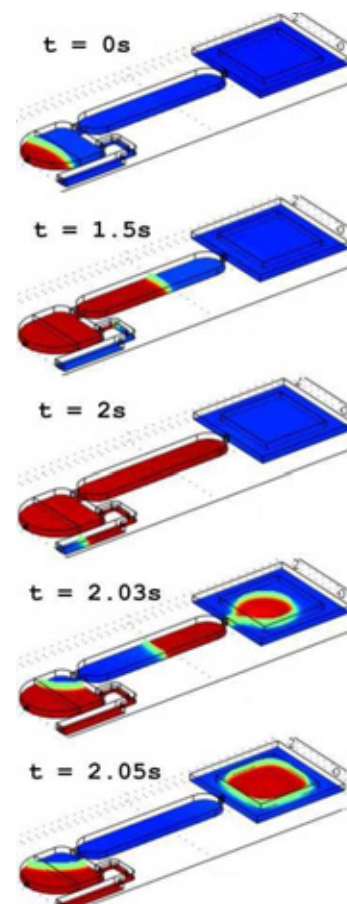


Figure 8. Cavity filling and droplet generation (water in red and air in blue).